Chapter 16

Radiation Response of Silicon Carbide Diodes and Transistors

Takeshi Ohshima, Shinobu Onoda, Naoya Iwamoto, Takahiro Makino, Manabu Arai and Yasunori Tanaka

Additional information is available at the end of the chapter

http://dx.doi.org/10.5772/51371

1. Introduction

Silicon Carbide (SiC) is regarded as a promising candidate for electronic devices used in harsh radiation environments (Rad-hard devices) such as in space, accelerator facilities and nuclear power plants [1-5]. In order to apply SiC to such rad-hard devices, we have to know the radiation response of the characteristics of SiC devices, because semiconductor devices show destructive and non-destructive malfunctions and/or degradation their characteristics due to irradiation. For radiation effects on semiconductor devices, three major effects, Single Event Effects (SEEs), Total Ionizing Dose (TID) effect, and Displacement Damage Dose (DDD) effects are known.

When charged particles such as heavy ions are irradiated into semiconductors, dense charge (electron-hole pairs) is generated in semiconductors along to the ion track. The malfunctions of electronic devices such as LSIs and power devices caused by charge generated by charged particles are called SEEs. The SEEs occur even by only one particle incidence, and there are both nondestructive (soft errors) and destructive (hard errors) SEE failures [6-8]. The soft errors arise if the amount of charge collected by devices is large enough to reverse or flip the data state of a memory cell, register, latch, or flip-flop. Since the soft errors are not destructive, the function of semiconductor devices can be recovered by writing new data to the bit and/or resetting of devices. For example, the Single Event Upset (SEU) and the Multiple Bit Upset (MBU) in a Static Random Access Memory (SRAM) and a Dynamic Random Access Memory (DRAM), the Single Event Functional Interrupt (SEFI) in Field Programmable Gate Array (FPGA) or DRAM control circuitry are known as the soft errors. Recently, the Single

Event Transient (SET) arises as a serious issue for analog electronics and digital logic cells. In general, the SETs in analog electronics are referred to as ASETs, and those in digital combinatorial logic are referred to as DSETs. In contrast, the Single Event Latch-up (SEL), the Single Event Burnout (SEB), and the Single Event Gate Rupture (SEGR) in power electronic devices are known as the hard errors.

Electron-hole pairs are induced in insulator layers of Metal-Insulator-Semiconductor (MIS) structure devices, such as Metal-Oxide-Semiconductor (MOS) devices by irradiation, and as a result, charge trapped in insulator (oxide) and/or traps near the interface between oxide and semiconductor (interface traps) are generated. Since such charge trapped in insulator and interface traps act give harmful influence to transport properties of semiconductors, the electrical characteristics of MIS devices are degraded by their generation [9, 10]. For example, the shift of threshold voltage (V_T) and the decrease in the channel mobility (μ_{ch}) are observed in MOS field effect transistors (FETs). This radiation effect is called the TID effect, and in general, the value of the TID effects gradually increases with increasing dose of radiations because the amount of radiation-induced charge in insulator and interface traps increases with increasing dose.

When energetic particles are irradiated into semiconductor crystals, atoms at lattice sites are scattered into non-lattice sites (knock-on effects). As a result, vacancies and interstitials are created in semiconductor crystals. This is the origin of the DDD effect. However, in reality, the structure of residual defects is not so simple and a wide variety of defects such as divacancies, vacancy clusters, and vacancy-impurity complexes exists in crystals because generated vacancies and interstitials thermally diffuse and finally they become stable defects. In general, such defects act as scattering/recombination centers to free carriers, and as a result, the electrical characteristics of semiconductors devices are degraded. In the case of the DDD effect, similar to the TID effect, the degradation of the characteristics of semiconductor devices becomes larger with increasing fluence of radiation. The degradation of the electrical performance of solar cells installed in space satellites is known as one of the examples of the DDD effect [11-14].

In this chapter, the effects of radiation on the electrical characteristics of SiC devices are described from the point of view of the TID effect and the SEEs.

2. Gamma-ray irradiation effects on SiC MOSFETs

Figure 1 shows the change in the subthreshold region of drain current (I_D) – gate voltage (V_G) curves (subthreshold curves) for n-channel 6H-SiC MOSFETs by gamma-ray irradiation. The bias of 12 V was applied to drain (V_D) during measurements. The gate oxide of the MOSFETs was formed using pyrogenic oxidation (H_2:O_2 = 1:1) at 1100°C. The mark „+“ on the each line indicates the value of V_T. As shown in the figure, the value of V_T shifts to the negative voltage side, and also the I_D-V_G curves stretches after irradiation. This suggests that charge in oxide and interface traps are generated by gamma-ray irradiation.

http://dx.doi.org/10.5772/51371

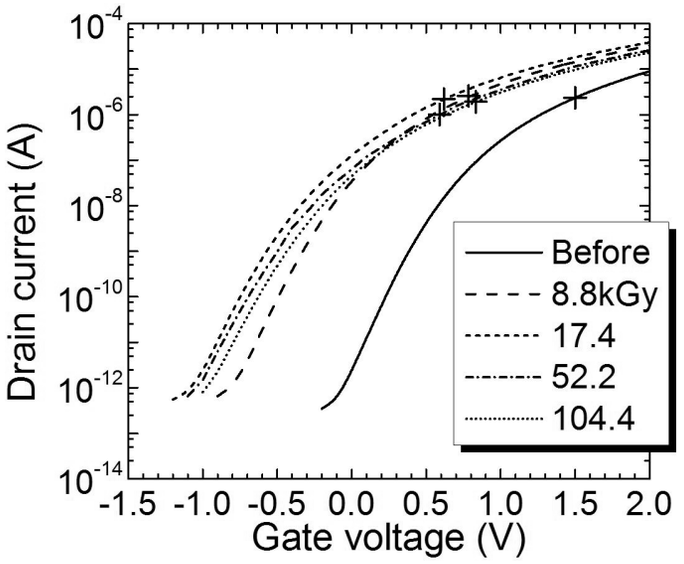

Figure 1. Change in the subthreshold region of I_D –V_G curves (subthreshold curves) for n-channel 6H-SiC MOSFETs by gamma-ray irradiation. The bias of 12 V was applied to drain during measurements. The „+" mark on the each line indicates the value of V_T.

According to Mcwhorter and Winokur [9], the density of charge trapped in gate oxide (ΔN_{OX}) and interface traps (ΔN_{IT}) generated by irradiation can be estimated from the shift of subthreshold curves using a following analysis. Since charge trapped in gate oxide does not respond to bias applied to gate, the entire subthreshold curve is simply shifted by the generation of charge trapped in gate oxide. On the other hand, since the charge state of interface traps depends on Fermi level (thus, the value of the bias applied to gate oxide), the subthereshold curve is stretched by the generation of interface traps. This behavior can be expressed as

$$\Delta V_T = \Delta V_{OX} + \Delta V_{IT} \tag{1}$$

where ΔV_T, ΔV_{OX} and ΔV_{IT} are the shift of the threshold voltage by irradiation, the voltage shifts due to the generation of oxide-trapped charge and interface traps, respectively. Also, since the charge state of interface traps is assumed to be neutral at midgap state, at which Fermi level corresponds to the intrinsic Fermi level, the shift of the midgap voltage (ΔV_{MID}) due to irradiation is caused by oxide-trapped charge. Thus,

$$\Delta V_{MID} = \Delta V_{OX} \tag{2}$$

Since the subthreshold curve between V_{MID} and V_T is stretched by the generation of interface traps, ΔV_{IT} is determined as

$$\Delta V_{IT} = \left(V_T - V_{MID}\right)_{post} - \left(V_T - V_{MID}\right)_{pre} \tag{3}$$

where „post“ and „pre“ mean after and before irradiation, respectively.

In order to obtain the value of V_{MID}, firstly, the drain current corresponding to the midgap condition (I_{MID}) is estimated. In the subthreshold region, I_D is expressed as the formula [15]

$$I_D = 2^{1/2}\mu\left(\mathrm{W}/\mathrm{L}\right)(\mathrm{q}N_A L_B/\beta)\left(n_i/N_A\right)^2\exp(\beta\phi_s)(\beta\phi_s)^{-1/2} \tag{4}$$

where N_A, n_i, ϕ_s and L_B are the acceptor (or donor) concentration in the channel region of a MOSFET, the intrinsic carrier concentration, band bending at the surface and the Debye length given by $L_B = (\varepsilon_s/(\beta q N_A))^{1/2}$, respectively. Here, β is equal to $q/k_B T$, where q and k_B are the electron charge and the Boltzmann constant, respectively. At the midgap condition, ϕ_s is equal to $(k_B T/q)\ln(N_A/n_i)$. Thus, I_{MID} can be estimated from eq. (4) using ϕ_s for $(k_B T/q)\ln(N_A/n_i)$. Then, the value of V_{MID} can be obtained from the value of V_G at I_{MID} on subthreshold curves. It should be mentioned that for the determination of V_{MID} for SiC, it is necessary to linearly extrapolate the lower position of the subthreshold curve down to the lower part of the curve, since the value of I_{MID} is of the order of 10^{-30} A.

The value of ΔN_{OX} and ΔN_{IT} is estimated from

$$\Delta N_{OX} = \Delta V_{OX}\ C_{OX}/q \tag{5}$$

$$\Delta N_{IT} = \Delta V_{IT}\ C_{OX}/q \tag{6}$$

where C_{OX} is equal to ε_{OX}/t_{OX}, and ε_{OX} and t_{OX} are the relative dielectric constant of SiO_2 and the thickness of gate oxide, respectively.

Figure 2 (a) shows the ΔV_T as a function of absorbed dose for n-channel 6H-SiC MOSFETs. The triangles, circles and squares represent results obtained from MOSFETs of which gate oxide was fabricated by dry (Dry) and pyrogenic (Pyro) oxidations at 1100°C and pryogenic oxidation followed by hydrogen annealing at 700°C for 30 min at a pressure of 20 Torr (H_2), respectively. For the details of the fabrication process of those MOSFETs, please see Ref. [16, 17]. For the Dry SiC MOSFETs, the ΔV_T slightly shifts to the positive voltage side above 50 kGy although the value does not change below 30 kGy. For the Pyro SiC MOSFETs, the value of ΔV_T shifts to the negative voltage side, and the negative shift become smaller above 30 kGy. For the H_2 SiC MOSFETs, the ΔV_T shows the negative shift around 20 kGy, however, the voltage shift terns to the positive above 30 kGy. Since the value of ΔV_T is affected by the generation of charge trapped in gate oxide and interface traps, for understanding the behavior of ΔV_T, it is necessary to know the information on ΔV_{OX} and ΔV_{IT}. Therefore, the value of ΔV_{OX} and ΔV_{IT} is derived from the subthreshold curves using Eqs. (1) – (4). The absorbed dose dependence of ΔV_{OX} and ΔV_{IT} is shown in Figs. 3 (a) and (b), respectively. The values of ΔV_{OX} for the Dry and the Pyro SiC MOSFETs show the negative voltage shift and the shift becomes large with absorbed dose. These results indicate that for the Dry and the Pyro SiC

http://dx.doi.org/10.5772/51371

MOSFETs, the positive charge is trapped in gate oxide by gamma-ray irradiation and the trapped charge increases with increasing absorbed dose. Since the shift of ΔV_{OX} for the Pyro SiC MOSFETs is larger than that for the Dry SiC MOSFETs, the value of trapped charge for the Pyro SiC MOSFETs is larger than that for the Dry SiC MOSFETs. On the other hand, ΔV_{OX} for the H_2 SiC MOSFETs shows complicated behaviors although the shift is very slight even after 530 kGy irradiation. Thus, firstly the ΔV_{OX} shifts to the negative voltage side at doses below 40 kGy. However, the value shows a positive voltage shift around 60 kGy although a negative shift appears at 180 kGy. Then, finally, the shift becomes positive again after irradiation at 530 kGy.

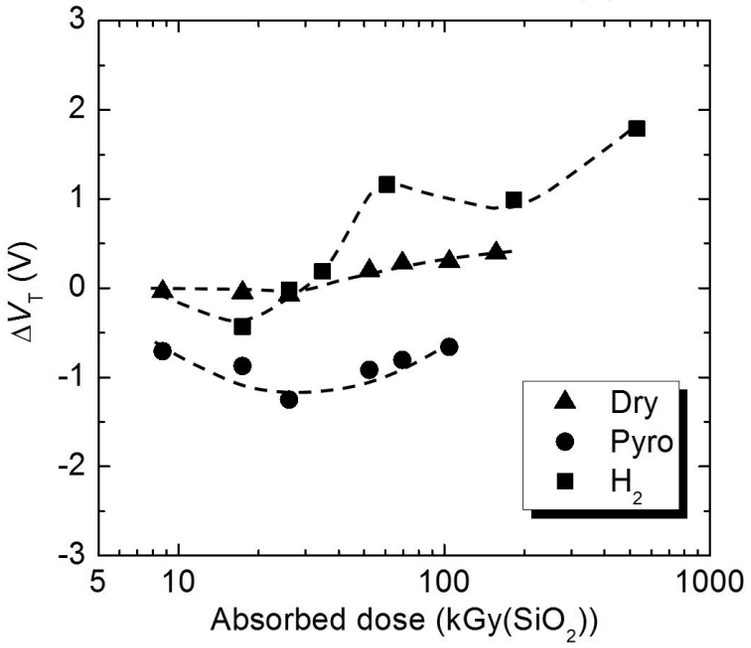

Figure 2. ΔV_T as a function of absorbed dose for n-channel 6H-SiC MOSFETs. The triangles, circles and squares represent results obtained from MOSFETs of which gate oxide was fabricated by dry (Dry) and pyrogenic (Pyro) oxidations at 1100°C and pryogenic oxidation followed by hydrogen annealing at 700°C for 30 min at a pressure of 20 Torr (H_2), respectively.

These behaviors indicate that both positively and negatively charges are generated in gate oxide for the H_2 SiC MOSFETs by gamma-ray irradiation. It was reported from the change in capacitance – voltage characteristics of 6H-SiC MOS capacitors due to gamma-ray irradiation that negative and positive trapped charges were generated near SiO_2/SiC interface and in oxide at 40 nm from the interface, respectively [18]. Although the mechanism of H_2-anneling effect on the gate oxide and the interface between oxide and SiC has not yet been clarified, since the initial value of V_T decreased by H_2 annealing [19], the large shift of ΔV_T to the positive voltage side and the unique behavior of ΔV_{OX} might occurs due to the reduction of H_2-annealing effects by gamma-ray irradiation. Also, it should be noticed that a part of interface traps might be detected as oxide-trapped-charge in this analysis since interface traps in the middle region of the band gap of 6H–SiC have extremely long charge release times at RT, and they act just as charge trapped in oxide [20]. In contrast to ΔV_{OX}, the values of ΔV_{IT}

for all SiC MOSFETs show the positive voltage side and their shifts become larger with increasing absorbed dose although the absolute values depend on the fabrication process of gate oxide, as shown in Fig. 3 (c).

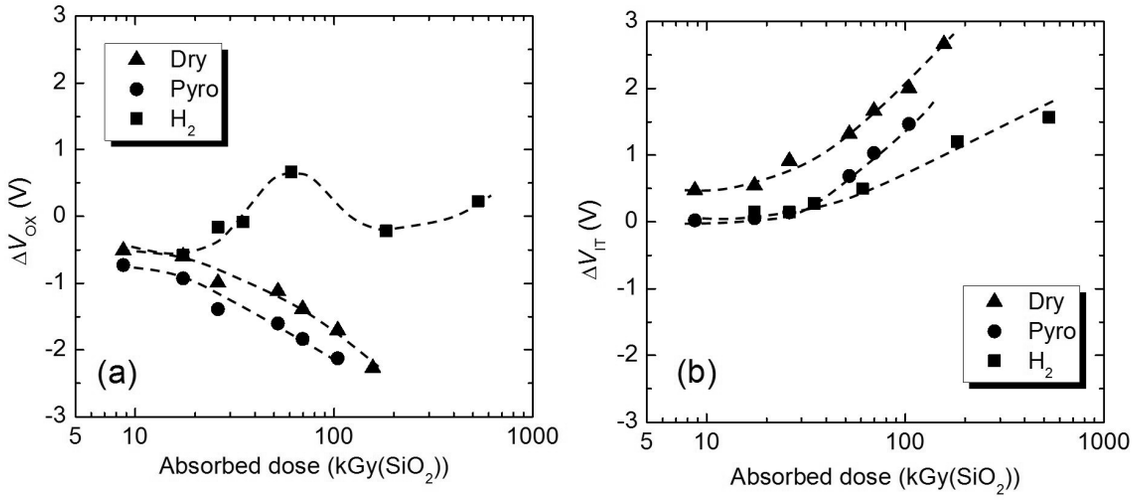

Figure 3. (a) ΔV_{OX} and (b) ΔV_{IT} as a function of absorbed dose for n-channel 6H-SiC MOSFETs. The triangles, circles and squares represent results obtained from MOSFETs of which gate oxide was fabricated by dry (Dry) and pyrogenic (Pyro) oxidations at 1100°C and pryogenic oxidation followed by hydrogen annealing at 700°C for 30 min at a pressure of 20 Torr (H_2), respectively.

The values of ΔN_{OX} and ΔN_{IT} are estimated from Figs. 3 (b) and (c), respectively, using Eq. (5)/(6). Figures 4 (a) and (b) show ΔN_{OX} and ΔN_{IT}, respectively, for the Dry (triangles), the Pyro (circles) and the H_2 (squares) SiC MOSFETs as a function of absorbed dose. For comparison, the reported results of Si MOSFETs are also plotted in the figures (upside-down triangles) [9]. The value of ΔN_{OX} for the Dry SiC MOSFETs is slightly smaller than that of the Pyro SiC MOSFETs and both values increase with increasing absorbed dose with an exponent of 2/3. It is also found that Si MOSFETs show the 2/3 power-low dependence, although the value of ΔN_{OX} for the Si MOSFETs is larger than that for the SiC MOSFETs [9]. On the other hand, the change in ΔN_{OX} for the H_2 MOSFETs due to irradiation show a different behavior from others, and the value is in order of 10^{11} /cm^2 even after irradiation at 530 kGy. These results indicate that the characteristics of gate oxide fabricated by H_2-annealing differ from those by non-annealing. However, it should be noticed that ΔN_{OX} estimated in this analysis is a value subtracting a positive component from a negative component. Thus, if both positive and negative components are almost the same value, the net number of ΔN_{OX} is small. Therefore, from this result, we cannot simply conclude that the quality of gate oxide fabricated by H_2-annealing is higher than that of gate oxide fabricated by non-annealing or not.

For ΔN_{IT}, the H_2 SiC MOSFETs have lower values than the other MOSFETs at absorbed doses above 30 kGy. The characteristics of SiC MOS devices were reported to be degraded by carbon related compounds remaining around the interface between SiO_2 and SiC [21]. Since such compounds might also act as precursors of radiation-induced interface traps, it is assumed that H_2 annealing to gate oxide of SiC MOSFETs reduces residual compounds near

the interface. For the absorbed dose dependence of ΔN_{IT}, the H_2 and the Dry SiC MOSFETs have the 2/3 power-low dependence although ΔN_{IT} for the Pyro SiC MOSFETs increases with increasing the absorbed dose with an exponent of approximately 3/2. The 2/3 power-law dependence is also reported in Si of which gate oxide was formed using dry oxidation [9]. The power-law dependence comes from the generation mechanism of interface traps, and the structural and/or electrical properties of the interface between SiO_2 and SiC for the H_2 and the Dry SiC MOSFETs are different from those for the Pyro SiC MOSFETs. Therefore, it is suggests that the characteristics of the interface between SiO_2 and SiC formed by pyrogenic oxidation followed by H_2-annealing are similar to those formed by dry oxidation.

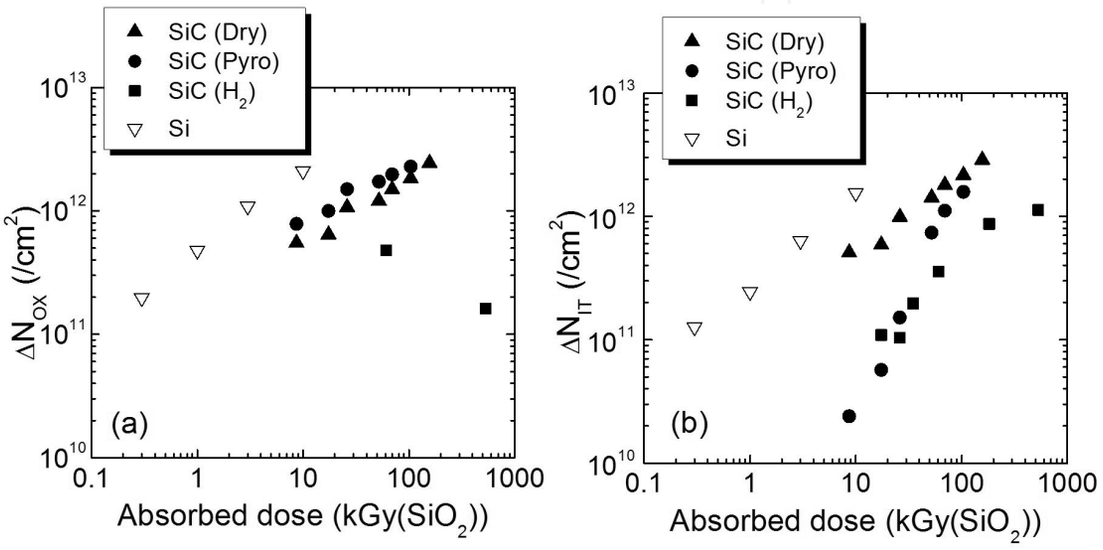

Figure 4. a) ΔN_{OX} and (b) ΔN_{IT} for Dry (triangles), Pyro (circles) and H_2 (squares) SiC MOSFETs as a function of absorbed dose. For comparison, the reported results of Si MOSFETs are also plotted in the figures (upside-down triangles) [9].

The μ_{ch} for Si MOSFETs is known to decrease with increasing absorbed dose [10]. In order to confirm this for SiC MOSFETs, μ_{ch} for the H_2 SiC MOSFETs were plotted as a function of absorbed dose (Fig. 5). For comparison, the result reported for Si MOSFETs are also plotted in the figure [9]. The μ_{ch} for the H_2 SiC MOSFETs does not change up to 20 kGy and the value decreases with increasing absorbed dose above 60 kGy. Then, the value of μ_{ch} reduces to be 50 % of the initial value at 530 kGy. On the other hand, μ_{ch} for the Si MOSFETs decreases with increasing absorbed dose and becomes 50 % of the initial value by irradiation at 10 kGy. Although the initial value of μ_{ch} for Si MOSFETs (600 cm^2/Vs) is much higher than the initial value of μ_{ch} for the H_2 SiC MOSFET (~ 50 cm^2/Vs), the value for Si MOSFETs is assumed to be almost zero after irradiation at 100 kGy whereas the H_2 SiC MOSFETs still keep 25 cm^2/Vs of μ_{ch} even after irradiation at 530 kGy. In addition, it is mentioned that the stability of their electrical performance against irradiation is also important for Rad-hard devices. Therefore, it can be concluded that SiC MOSFETs are quite tolerant against radiation in comparison with Si MOSFETs. For the degradation mechanism of μ_{ch}, Ohshima et al. reported [17] that the relationship between the decrease of μ_{ch} and ΔN_{IT} for SiC MOSFETs was described by the same relationship reported for Si MOSFETs ($\mu_{ch} = \mu_0 /(1 + \alpha \Delta N_{IT})$) [10], where μ_0

and α are the initial value of the channel mobility and a constant (= 7.0±1.3×10^{-13}), respectively. This suggests that μ_{ch} for SiC MOSFETs as well as Si MOSFETs can be explained in term of carrier scattering in the channel region by interface traps generated by gamma-ray irradiation. Since interface traps located in the middle of the band gap behave just like charge trapped oxide for SiC, ΔN_{IT} obtained in this analysis means the net density of interface traps which act as carrier scattering centers. It was reported that the channel mobility of 6H–SiC MOSFETs is affected by acceptor-like traps existing near the conduction band edge [22]. Although the relationship between interface traps induced by irradiation and intrinsic interface traps has not yet been clarified in the case of SiC MOS devices, it is assumed that the radiation resistance of SiC MOSFETs might be improved by the reduction of initial interface traps generated near the conduction band edge.

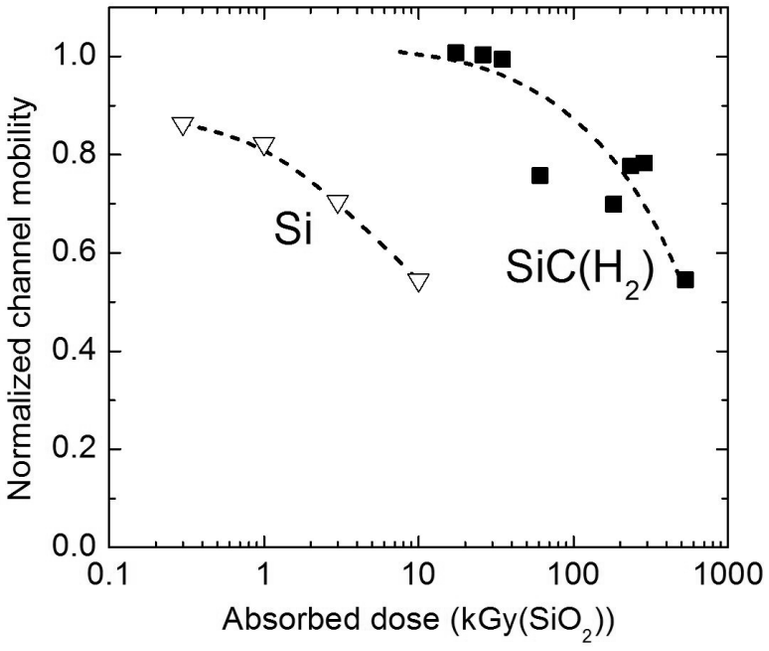

Figure 5. μ_{ch} for H_2 SiC MOSFETs as a function of absorbed dose. For comparison, the result reported for Si MOSFETs are also plotted in the figure [9]. The value of the channel mobility is normalized by the initial value.

Next, the effects of the surface morphology on μ_{ch} of SiC MOSFETs irradiated with gamma-rays will be discussed. In this study, MOSFETs were fabricated on n-type 6H-SiC epitaxial layers using the same fabrication process except the procedures of high temperature annealing after implantation [23]. Thus, although all samples were annealed at 1650°C for 3 min in an Ar atmosphere, the surface of one series of samples was covered with carbon films (C-coating) during the annealing to avoid the degradation of the surface morphology [24], and the other series of samples were annealed without the carbon coating (non-coating). After the annealing, the carbon films were removed by the oxidation at 800°C for 30 min in O_2 gas. Gate oxide of both series of the MOSFETs were formed by pyrogenic oxidation (H_2:O_2 = 1:1) at 1100°C for 30 min. For the details of the fabrication process, please see Ref. [23]. The initial values of μ_{ch} for C-coating and non-coating SiC MOSFETs are 41 and 44 cm^2/Vs, respective-

http://dx.doi.org/10.5772/51371

ly. For the surface morphology, the values of root mean square (RMS) for the C-coating and non-coating SiC are obtained to be 0.67 and 1.36 nm, respectively, from AFM measurements, whereas the RMS was 0.25 nm before annealing.

Figures 6 (a) and (b) show μ_{ch} and ΔN_{IT}, respectively, for C-coating (squares) and non-coating (circles) SiC MOSFETs as a function of absorbed dose. As shown in the figure, no significant decrease or slight increase in μ_{ch} is observed for the C-coating SiC MOSFETs. The value of ΔN_{IT} for the C-coating SiC MOSFETs is estimated to be less than $4x10^{11}$ /cm^2, and no significant increase in ΔN_{IT} is observed up to 3 MGy. In contrast, μ_{ch} for the non-coating SiC MOSFETs decreases with increasing absorbed dose above 2 MGy. In the absorbed region that μ_{ch} decreases, ΔN_{IT} increases with increasing absorbed dose, and the value becomes of the order of 10^{12} /cm^2 by irradiation above 2 MGy. As above-mentioned, μ_{ch} is degraded by the generation of interface traps. Therefore, the decrease in μ_{ch} for the non-coating SiC MOSFETs can be interpreted in terms of the generation of interface traps. Also, it was reported by Kimoto [24] the channel mobility can be affected by the surface roughness. So, the higher radiation resistance obtained for the C-coating SiC MOSFETs compared to non-coating ones is caused by the less surface roughness.

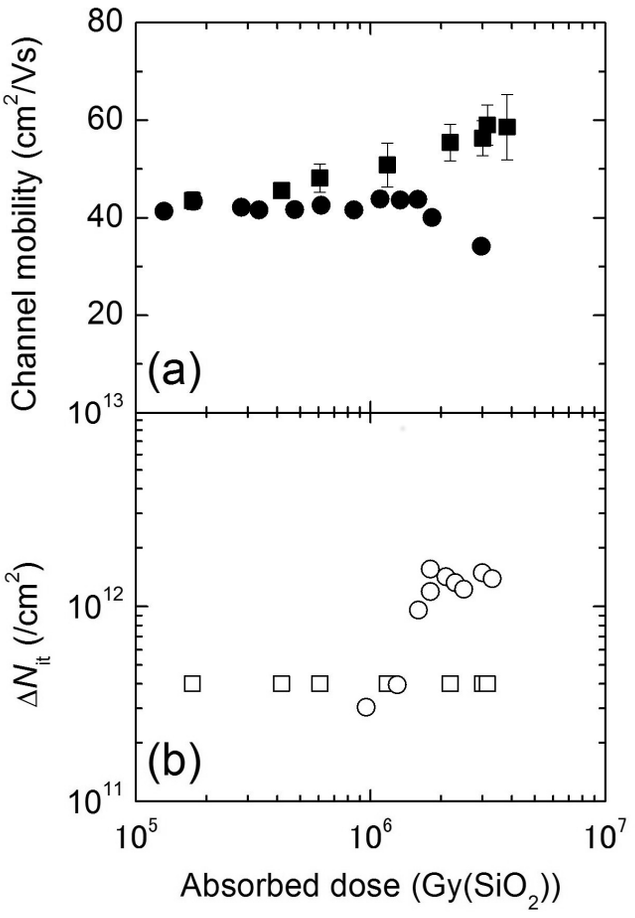

Figure 6. a) μ_{ch} and (b) ΔN_{IT} for C-coating (squares) and non-coating (circles) SiC MOSFETs as a function of absorbed dose.

3. Radiation hardness of SiC devices

In this section, the change in the electrical characteristics of SiC transistors such as Static Induction Transistors (SITs), Metal-Semiconductor (MES) FETs and MOSFETs due to gamma-ray irradiation will be compared to Si MOS FETs from the point of view of the radiation hardness. Figure 7 shows ΔV_T for SiC SITs [25], SiC MESFETs [26], C-coating+Dry SiC MOSFETs and C-coating+Pyro SiC MOSFETs as a function of absorbed dose. All transistors were irradiated with gamma-rays at RT. During gamma-ray irradiation, no bias was applied to any electrodes of the transistors. For comparison, the results reported for Si MOSFETs are also plotted in the figure [9]. No significant change in ΔV_T for All SiC transistors is observed up to 10^5 Gy whereas the Si MOSFETs show obvious degradation in ΔV_T. This indicates that those SiC transistors have extremely high radiation resistance compared to the Si MOSFETs. The value of ΔV_T for both the SiC MOSFETs shifts to the negative voltage side in high dose regions, and the shift for the C-coating+Dry ones is larger than that for the C-coating+Pyro ones. Thus, the C-coating+Pyro MOSFETs have higher radiation resistance than the C-coating+Dry MOSFETs. For the SiC MESFETs, the shift of ΔV_T to the negative voltage side increases with increasing in absorbed doses regions between 4×10^5 and 2×10^6 Gy, and the maximum shift of -0.75 V is observed at 2×10^6 Gy. However, the negative shift becomes smaller with increasing absorbed dose above 3×10^6 Gy and the value of ΔV_T becomes -0.27 V after irradiation at 10^7 Gy. For the SiC SITs, although the positive shift is observed for ΔV_T above 10^6 Gy, the value is relatively small (0.45V at 7×10^6 Gy) compared to other SiC transistors. Thus, it can be concluded that the radiation hardness of the SiC SITs and the MESFETs is higher than that of the SiC MOSFETs. Since SITs and MESFETs do not have gate oxide, such high radiation resistance to gamma-rays can be observed. However, it should be noticed that the characteristics of SiC SITs and MESFETs are also affected by TID effects since the SiC SITs and the MESFETs is covered with a insulator (oxide) for the surface termination, and charge is trapped in such insulator. In addition, in such a high absorbed dose region, the displacement damage effect by Compton electrons also occurs and the characteristics of devices are degraded.

Next, the change in the electrical characteristics of the SiC SITs by gamma-ray irradiation is expressed. The SiC SITs have an on-resistance of 0.15 Ω and a blocking voltage of 900 V at V_G of -10 V before irradiation [27, 28]. Since the SiC SITs were developed as power devices, two Si power devices with similar current and voltage ratings, Si MOSFET (17N80C3) and Si IGBT (5J301), were also irradiated with gamma-rays for comparison. The SiC SITs mounted in TO220 packages were irradiated with gamma-rays at absorbed dose rate of 8.8 kGy/h at RT. During irradiation, no bias was applied to electrodes. The shift of the breakdown voltage for the SiC SITs (squares), the Si MOSFETs (triangles) and the Si IGBT (upside-down triangles) as a function of absorbed dose is shown in Fig. 8. The blocking characteristics for the SiC SITs and the Si ones (IGBTs and MOSFETs) were measured under V_G at 10 V and 0V, respectively. No significant change in the breakdown voltage for the SiC SITs and the Si IGBT is observed up to 10^7 Gy. For the Si MOSFETs, the shift of the breakdown voltage increases with absorbed dose above 4×10^5 Gy, and the large shift of -500 V is observed at 10^7 Gy. It was also reported [25] that no significant increase in the leakage current for the SiC SITs (of the order of 10^{-6} A) was observed where the leakage current for the Si MOSFETs increased to 10^{-4} A level after irradiation 10^7 Gy.

http://dx.doi.org/10.5772/51371

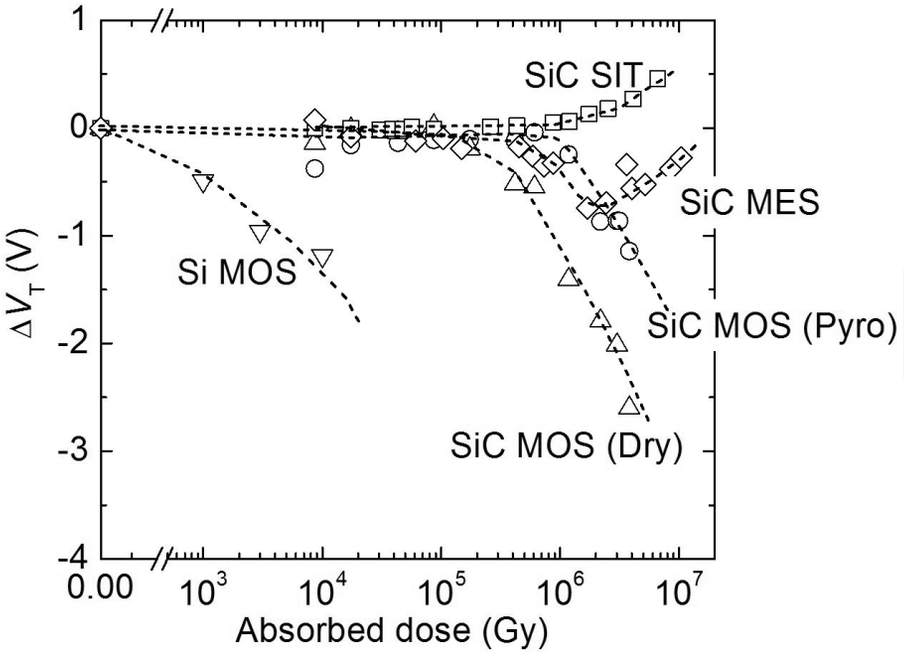

Figure 7. Change in ΔV_T for SiC SITs (squares), SiC MESFETs (diamonds), C-coating+Dry SiC MOSFETs (triangles) and C-coating+Pyro SiC MOSFETs (circles) as a function of absorbed dose. All transistors were irradiated with gamma-rays at RT. During gamma-ray irradiation, no bias was applied to any electrodes of the transistors. For comparison, the results reported for Si MOSFETs (upside-down triangles) are also plotted in the figure [9].

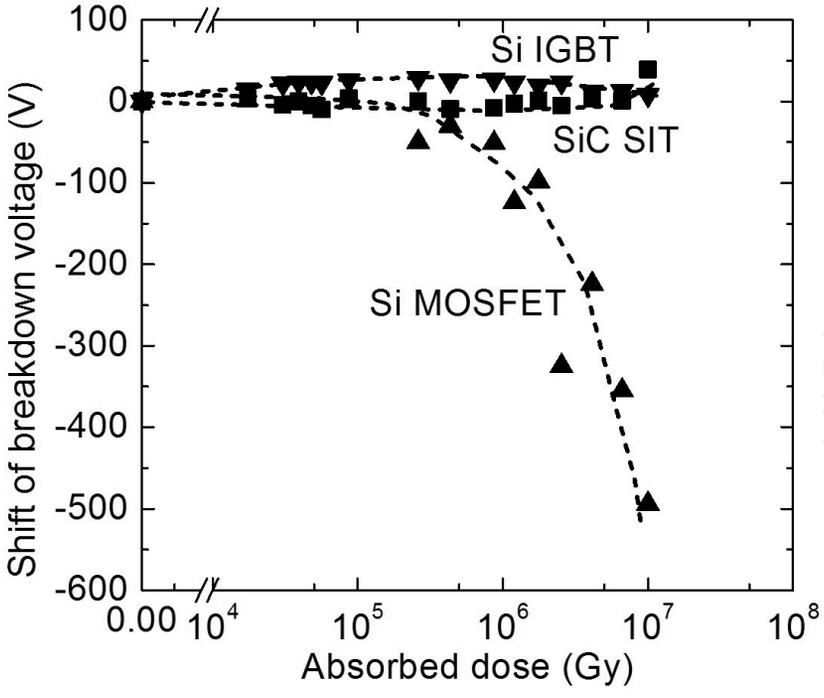

Figure 8. Shift of the breakdown voltage from the initial value for SiC SITs (squares), Si MOSFETs (triangles) and Si IGBT (upside-down triangles) as a function of absorbed dose. The blocking characteristics for SiC SITs and Si ones (IGBTs and MOSFETs) were measured under V_G at 10 V and 0V, respectively.

The on-state characteristics were measured under V_G at +2.5 V for the SiC SITs and at +15 V for the Si transistors (IGBTs and MOSFETs). Then, the on-voltage was defined as the value of V_D at I_D of 10 A. Figure 9 shows the shift of the on-voltage for the SiC SITs (squares), the Si MOSFETs (triangles) and the Si IGBT (upside-down triangles) as a function of absorbed dose. The shift of on-voltage for the SiC SITs and the Si MOSFETs due to gamma-ray irradiation shows a very stable behavior up to 10^7 Gy, whereas the on-voltage for the Si IGBTs remarkably increases after irradiation at 8×10^5 Gy (from 2.3 to more than 20 V). It was reported [29] that the displacement damage effect induced by Compton electrons degrades the gain for Si bipolar transistors. So, the result obtained from the Si IGBT is interpreted in terms of the majority carrier removal in the drift region (low doping region) due to the displacement damage effect. For the SiC SITs and the Si MOSFETs, since the doping concentration in the drift region is not low, the displacement damage effect might not be observed and as a result, on-voltage shows almost constant values up to 10^7 Gy. Although the stable on-voltage behavior is obtained for the SiC MOSFETs, the large fluctuation of V_T was reported due to the TID effect. Considering gamma-ray irradiation effects on the breakdown voltage, the on-voltage, and V_T, the characteristics of only the SiC SITs show the stable behaviors up to 10^7 MGy. Thus, we can conclude that the SiC SITs have extremely high radiation resistance, they have an enough potential for electronic devices used in harsh radiation environments such as nuclear power plants, space, and so on.

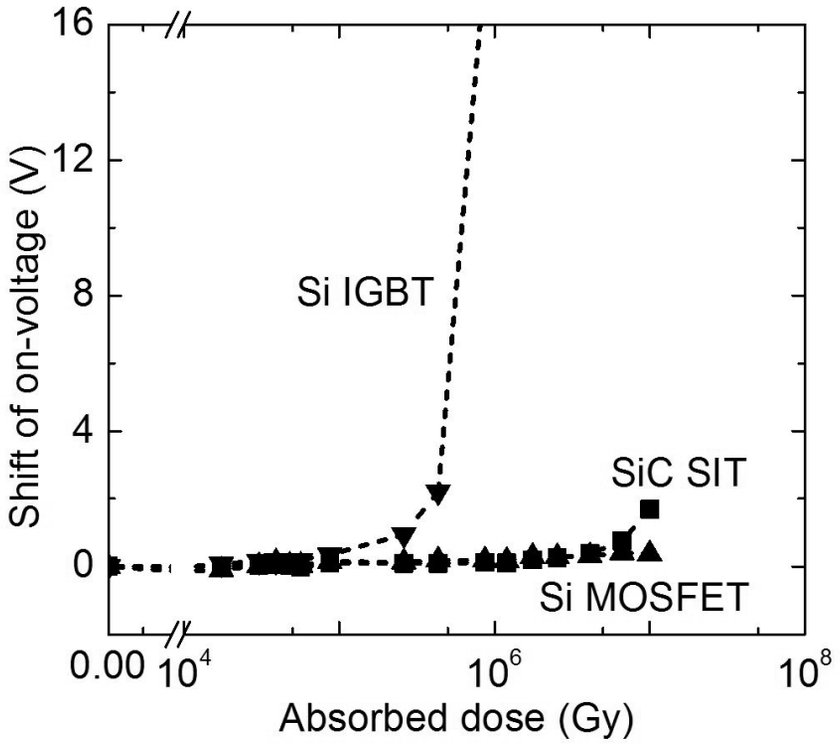

Figure 9. Shift of the on-voltage from the initial value for SiC SITs (squares), Si MOSFETs (triangles) and Si IGBT (upside-down triangles) as a function of absorbed dose.

http://dx.doi.org/10.5772/51371

4. Charge induced in SiC diodes by Ion irradiation

Since destructive or/and non-destructive malfunctions called SEEs occurs in electronic devices by charge (electron-hole pairs) generated by charged particle incidence, especially heavy ions. The SEEs on semiconductor devices are one of the most major issues for space applications. On the other hand, for high energy physics using accelerators with high luminosity, such as J-PARC and Super-LHC, Rad-hard particle detectors are expected to be developed. For the development of Rad-hard particle detectors as well as Rad-hard devices for space applications, it is important to clarify the behavior of charge generated in devices by charged particle incidence. In a previous study [30], Nava et al. reported that the Charge Collection Efficiency (CCE) obtained from 4H-SiC Schottky diodes by alpha particle incidence was estimated to be 100 %. It was also reported that 4H-SiC Schottky diodes could detect X-rays from radio isotopes [31,32]. Besides, the neutron detection by SiC diodes was investigated previously [33, 34]. As for light ions and X-rays irradiation into SiC, relatively large number of studies has been already reported. On the other hand, from the point of view of SEEs, study of ion irradiation on electronic devices using heavy ions is important. In this section, charge induced in SiC diodes by heavy ion incidence is reviewed on the basis of our previous studies [35-40].

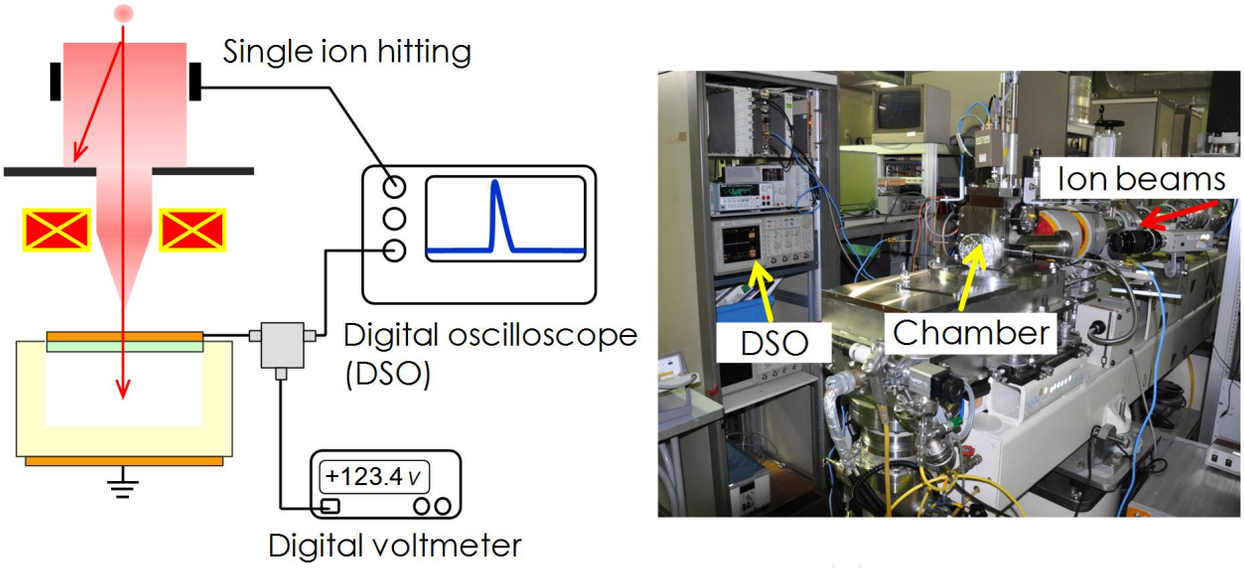

Figure 10. Schematic set-up of the TIBIC system installed at JAEA Takasaki and photo of the TIBIC system.

In order to obtain the information on charge induced in electronic devices, Ion Beam Induced Charge (IBIC) measurements is thought to be one of the useful methods. However, the decrease in collected charge during IBIC measurements should be considered for the accurate evaluation of charge induced by ion beams, since the device characteristics are degraded by radiation damage created in samples by ion incidence [41]. Therefore, single-ion hit Transient Ion Beam Induced Current (TIBIC) was developed at JAERI Takasaki in order to realize the evaluation of ion-induced current with minimizing the influence of damage

[42]. Figure 10 shows the schematic set-up of the TIBIC system installed at JAEA Takasaki and the photo of the TIBIC system. The TIBIC collection system connects with a heavy ion microbeam line from the 3MV Tandem accelerator, and consists of a single event triggering system and a fast switch beam shutter system. The transient current signals induced by ions can be detected using a digital sampling oscilloscope (Tektronix 3 GHz TDS694C or 15 GHz TDS6154C). The details of the single ion hit TIBIC collection system are described in Ref. [43]. Since the TIBIC system connects with a beam scanning system, spatial images of transient current signals can be obtained.

Figure 11 shows TIBIC signals obtained from 6H-SiC n^+p diodes with applied bias of 30, 90 or 150 V. Si ions with 12 MeV were used as probe beams. In this study, the 6H-SiC n^+p diodes with 100 - 300 μm diameters were fabricated on p-type substrates with p-type epitaxial layers (Al doping concentration between $8x10^{14}$ and $3.5x10^{15}$ /cm^3). The n^+ region was formed by three-fold implantation (60, 90, 140 keV) of phosphorus (P) ions at 800°C and subsequent annealing at 1650°C for 3 min in argon (Ar) atmosphere. The thickness and a mean P concentration of the implanted layer are ~100 nm and $5x10^{19}$ /cm^3, respectively. During the annealing, the sample surface was covered with a carbon film to avoid the degradation of the surface morphology [24]. The details of the diode fabrication process are described elsewhere [40]. The peak height of the TIBIC signals increases with increasing applied bias, and the value becomes to 0.50 from 0.19 mA when applied bias increases to 150 from 30 V. The fall-time, which is defined as the time from 90 % to 10 % of the current transient, shorten with increasing applied reverse bias, and the value decreases to 0.48 from 0.98 ns when applied bias increases to 150 from 30 V. These results can be interpreted in terms of an increase of the electric field in the depletion layer due to increasing applied bias. It is also mentioned the leakage currents of the diodes were in order of 10^{-11} A at an applied reverse bias of 150 V, and no significant differences in *I -V* characteristics between before and after TIBIC measurements were observed.

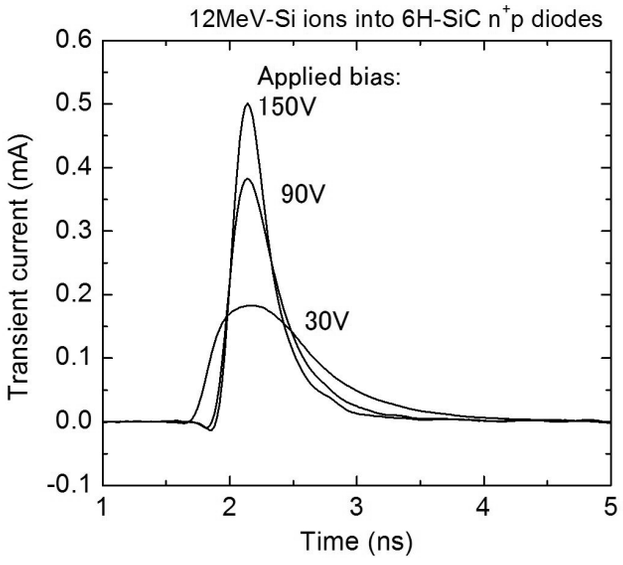

Figure 11. TIBIC signals obtained from 6H-SiC n^+p diodes with applied bias of 30, 90 or 150 V. Si ions with 12 MeV were used as probe beams.

http://dx.doi.org/10.5772/51371

By the integration of a TIBIC signal, charge collected by a diode can be estimated. Charge collected by the 6H-SiC n^+p diodes as a function of applied bias is shown in Fig. 12. In this study, Si ions with different energies were applied as probe beams, and the value of energy of Si ions are described in the figure. Charge collected by the diodes increases with increasing applied bias, and the value of collected charge saturates in a higher bias region. For example, the saturation is observed above 40 and 60 V for 15 and 18 MeV, respectively. Charge generated in the depletion region of a diode can be collected by its electric field (Drift component). On the other hand, charge generated in deeper than the depletion region diffuses, and only charge reaching the repletion region can be collected by a diode (Diffusion component) whereas some generated carriers recombine during diffusion. Thus, if the depletion region is shorter than the projection range of ions, the decrease in collected charge is observed due to the recombination of generated carriers during diffusion. Since ions with higher energy have a longer projection range, the results obtained in Fig. 12 can be qualitatively interpreted in terms of the drift and the diffusion components. However, in reality, since an extended drift region is temporarily created in a deeper region than the depletion region, the saturation of collected charge occurs even in the case that the depletion region is shorter than the ion projection range [44].

At a bias of 150V, the depletion region is estimated to be 7 μm, and this is longer than the ion projection range of Si ions at 18 MeV which is estimated to be 4.8 μm by a Monte Carlo simulation code, SRIM [45]. Thus, at a bias of 150 V, all charge generated in the 6H-SiC diodes by Si ion incidence can be collected by the electric field in the depletion layer. The CCE for the 6H-SiC diodes is estimated from the value of charge collected at a bias of 150 V. Here, the value of CCE is defined as

$$\left(Q_{exp} / Q_{ideal}\right) \text{ x } 100 \tag{7}$$

where Q_{exp} and Q_{ideal} are the value of charge experimentally obtained at 150 V and the ideal value of charge generated in SiC, respectively. The value of Q_{ideal} is obtained by the equation

$$Q_{ideal} = \left(E_{ion} / E_{e-h}\right) \text{ x} e \tag{8}$$

where E_{ion}, $E_{e\text{-}h}$ and e are the energy of incident ions, the generation energy of an electron-hole (*e-h*) pair and electron charge, respectively. In this study, the value of $E_{e\text{-}h}$ in 6H-SiC is assumed to be 7.8 eV (= 2.8Eg) on the analogy of $E_{e\text{-}h}$ in Si because the value of the energy for 6H-SiC has not been determined yet. It should be mentioned that the energy loss in the top Al electrode, the n^+ region and by non-ionizing collisions and also the decay of signal in the measurement system are not considered in this estimation, and the reduction of the CCE due to those effects is estimated to be between 8 and 14 %. The value of the CCE for the SiC n^+p diodes probed by Si ions at energies of 6, 12, 15 and 18 MeV is estimated to be 74, 83, 86

and 88 %, respectively. Since the effect of the energy loss in the Al electrode and the n^+ region on the reduction of the CCE value decreases with increasing ion energy, the experimental result that higher CCE value is observed by higher energy ion incidence is reasonable. However, even after considering energy loss in those regions, the value of the CCE for 6MeV is not comparable to that for 12, 15 and 18 MeV. This suggests that the CCE is degraded by another effect in the case of 6 MeV-Si.

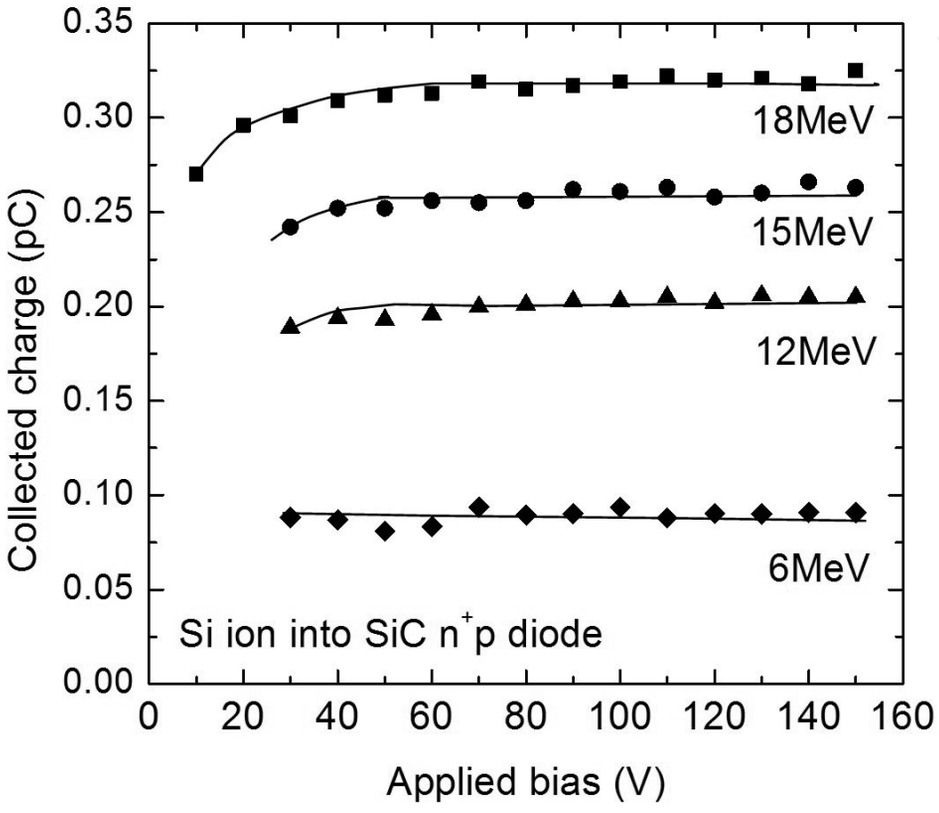

Figure 12. Charge collected by 6H-SiC n^+p diodes as a function of applied bias. Si ions with different energies were applied as probe beams, and the value of energy of Si ions are described in the figure.

In order to understand the degradation of the CCE due to not energy loss near the surface regions, the effect of ion species on the CCE was investigated. Figure 13 shows the relationship between ions species with the same energy (12 MeV) and the value of the CCE. The value of the CCE is obtained from the integration of TIBIC signals for the 6H-SiC n^+p diodes at a bias of 150 V. The CCE for the diodes probed by O ions is estimated to be 90 %, and this value is the highest of all ion species in Fig. 13. With increasing atomic number, the value of the CCE decreases. The CCE of 42 % is observed by Au ion incidence. The degradation of the CCE for SiC diodes by Au ion incidence was also reported [36]. Zajic et al. suggested that high density of e-h pairs is generated by heavy ions, and generated e-h pairs are easy to recombine in such dense plasma [46].

http://dx.doi.org/10.5772/51371

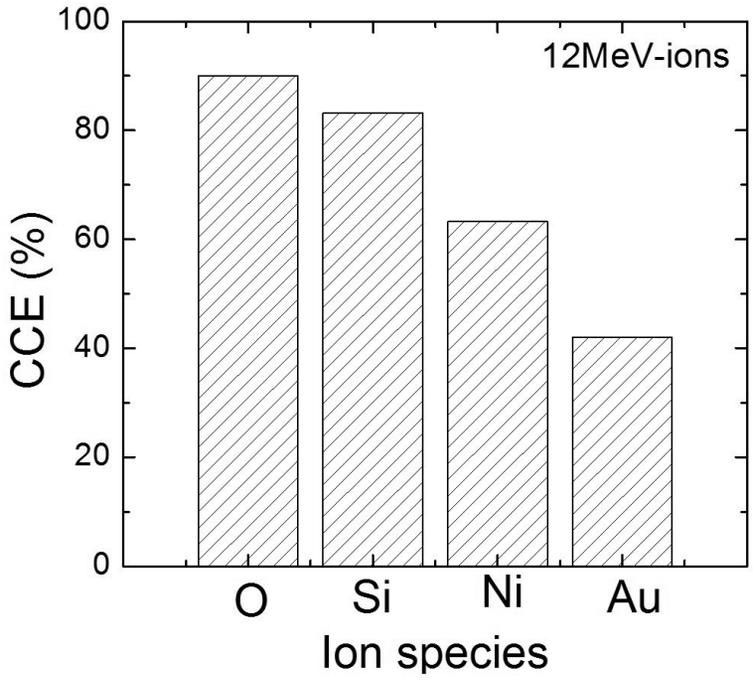

Figure 13. Relationship between ions species with the same energy (12 MeV) and the value of CCE. The value of CCE is obtained from the integration of TIBIC signals for 6H-SiC n^+p diodes at a bias of 150 V.

The carrier density generated in SiC, and the distributions of e-h pairs are calculated on the basis of Kobetich and Katz (KK) theorem [47]. In this calculation, the KK model improved using empirical equations reported by Fageeha et al. [48] was applied since the KK model overestimates the density of e-h pairs at the core of the ion track. The calculated results of the density of e-h pairs generated in SiC by (Left) 12 MeV-O and (Right) -Au ion irradiation are shown in Fig. 14. In the case of 12 MeV-O ion incidence, the radius of the ion track at the sample surface and projection range of ions are estimated to be ≈ 40 nm and 5.2 μm, respectively. On the other hand, the ion track radius at the surface and the ion range for 12 MeV-Au ions are estimated to be ≈ 2 nm and 1.9 μm, respectively. Since the energy (12 MeV) is the same for both O and Au ions, the total number of e-h pairs generated in the ion track region is the same between O and Au ions. Thus, the density of e-h pairs in SiC irradiated with Au ions is much higher than that irradiated with O ions, and the estimated density of e-h pairs in SiC irradiated with 12 MeV-Au ions is a several orders of magnitude higher than that in SiC irradiated with 12 MeV-O ions. In such a high density of e-h pairs, the ambipolar effect occurs easily and the electric field temporarily weakens. As a result, the amount of the recombination between electrons and holes increases. For the dynamics of carriers generated in SiC by heavy ion incidence, please see Ref. [44]. The result obtained in this study indicates that it is important to consider the decrease in the CCE for SiC particle detectors when heavy ions are detected. From the point of view of SEEs in SiC, the decrease in collected charge is thought to be one of the advantages for the development of Rad-Hard devices. The similar charge collection behaviours have been also obtained for SiC p^+n diodes, although only results obtained from SiC n^+p diodes were introduced in this article [39].

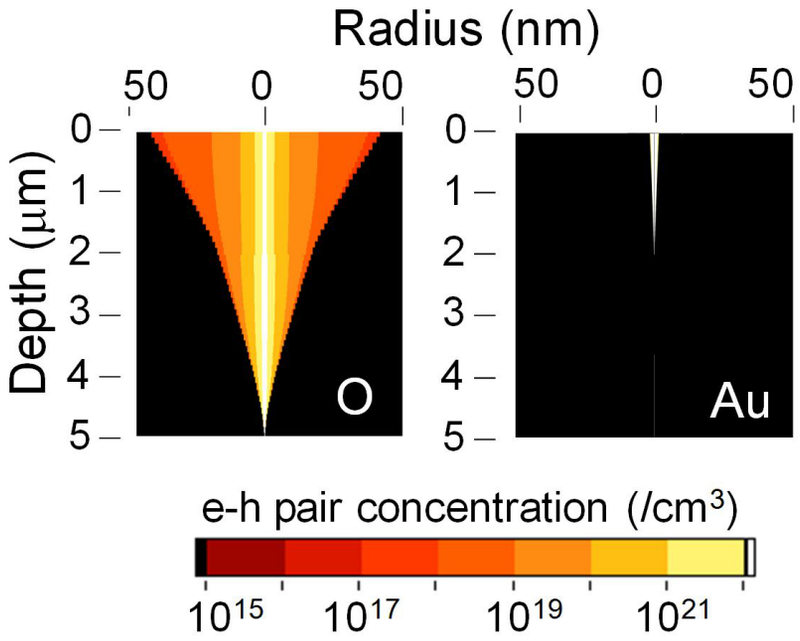

Figure 14. Calculated results of the e-h density generated in SiC by (Left) 12 MeV-O and (Right) -Au ion irradiation.

For the effects of ion incidence on MOS capacitors fabricated on SiC, it was reported that the peak amplitude of TIBIC signals decreased and the fall time increased with increasing number of incident ions [49-51]. Furthermore, the peak of TIBIC signals can be refreshed to its original value by applying a forward bias of + 1V to the gate electrode. From the measurement of the capacitance of SiC MOS capacitors during O ion irradiation, the value of capacitance was found to increase with increasing number of incident ions. This indicates that the depletion length of the MOS capacitors becomes shorten with increasing number of incident ions. Since large amounts of charge are induced by heavy ion incidence and some of them might flow to the interface between SiO_2 and SiC, the degradation of TIBIC signals can be explained by a change in the net bias applied to the gate oxide due to the creation of the inversion region or/and charging up deep traps. The refreshment of TIBIC signals by applying a forward bias can be also interpreted in terms of releasing charge from the interface or/and deep traps. For the effects of heavy ion irradiation on 6H-SiC MOSFETs, Onoda et al. Reported from experimental results and their simulation using the Technology Computer Aided Design (TCAD) [52] that the charge collection behaviours were affected by drift, funnelling, diffusion, and recombination, and especially, the enhancement of transient currents was observed due to the parasitic bipolar action. It was also reported that the enhanced charge collection was observed for 4H-SiC MESFETs by heavy ion incidence [26]. According to device simulations using the TCAD, it was concluded that the enhanced charge collection effect can be interpreted in terms of not only the bipolar action but also the channel modulation effects. For the DDD effect in SiC devices, it was reported that the value of the CCE for SiC n^+p diodes and the majority carrier concentration in them decreased with increasing gamma-rays, electrons or protons and the damage factor of the CCE and the carrier removal rate can be scaled by Non Ionizing Energy Loss (NIEL) [53-55].

http://dx.doi.org/10.5772/51371

5. Summary

In order to develop Rad-hard devices based on SiC, the radiation response of SiC devices have to be understood. In this chapter, effects of gamma-rays and swift heavy ions on SiC devices were reviewed. Firstly, the gamma-ray irradiation effects on SiC MOSFETs were introduced, and the degradation of their characteristics was discussed on the basis of charge generated in gate oxide and interface traps by irradiation. Then, the radiation resistance of SiC transistors, MOSFETs, MESFETs and SITs was compared to Si transistors. SiC transistors showed higher radiation resistance than Si transistors, and SiC SITs could be operated up to 10 MGy. This indicates that SiC SITs have extremely high radiation tolerance from the point of view of TID effects. Charge generated in 6H-SiC n^+p diodes by heavy ion incidence was evaluated using TIBIC. The signal peak of the transient current increased, and the fall-time decreased with increasing applied reverse bias. The high CCE values were observed when ions with relatively light mass such as O and Si ions were applied as probe ions. However, the CCE decreased with increasing atomic number, and the value reduced to approximately 40 % when 12 MeV-Au ions were applied as probe ions. From the calculation based on the modified KK model, it was found that the density of e-h pairs in SiC irradiated with heavy ions, such as Ni and Au, is much higher than that in SiC irradiated with O and Si ions. Therefore, the decrease in the CCE by the irradiation of ions with heavy mass was interpreted in terms of the recombination of e-h pairs in plasma.

Acknowledgements

This study of gamma-ray irradiation effects on SiC SIT was supported by the Strategic Promotion Program for Basic Nuclear Research by the Ministry of Education, Culture, Sports, Science and Technology of Japan. Also, the study of charge induced in SiC pn diodes and MOS capacitors by heavy ion incidence was partially supported by the Ministry and Education, Science, Sports and Culture, Grant-in-Aid for Scientific Research (B), 2006, 18360458 and (B), 2009, 21360471, respectively.

Author details

Takeshi Ohshima[1*], Shinobu Onoda[1], Naoya Iwamoto[1], Takahiro Makino[1],
Manabu Arai[2] and Yasunori Tanaka[3]

*Address all correspondence to: ohshima.takeshi20@jaea.go.jp

1 Japan Atomic Energy Agency (JAEA), Japan

2 New Japan Radio Co., Ltd. (NJRC), Japan

3 National Institute of Advanced Industrial Science and Technology(AIST), Japan

References

[1] Ohshima, T., Yoshikawa, M., Itoh, H., Takahashi, T., Okumura, H., Yoshida, S., & Nashiyama, N. (1996). Effects of Gamma-ray Irradiation and Thermal Annealing on Electrical Characteristics of SiC MOSFETs. Inst. *Phys. Conf. Ser.*, 142, 801-804.

[2] Ohshima, T., Yoshikawa, M., Itoh, H., Aoki, Y., & Nashiyama, I. (1998). Generation of Interface Traps and Oxide-Trapped Charge in 6H-SiC Metal-Oxide-Semiconductor Transistors by Gamma-ray Irradiation. *Jpn. J. Appl. Phys.*, 37, L 1002-L1004.

[3] Lee, K. K., Ohshima, T., & Itoh, H. (2002). Radiation Response of p-Channel 6H-SiC MOSFETs Fabricated Using Pyrogenic Conditions. *Materials Science Forum*, 389-393, 1097-1100.

[4] Nishijima, T., Ohshima, T., & Lee, K. K. (2002). Investigation of the Radiation Hardness on Semiconductor Devices using the Ion Micro-Beam. *Nucl. Instrum. Meth. B*, 190, 329-334.

[5] Lee, K. K., Ohshima, T., & Itoh, H. (2003). Performance of Gamma Irradiated p-Channel 6H-SiC MOSFETs: High Total Dose. *IEEE Trans. Nucl. Sci.*, 50, 194-200.

[6] Binder, D., Smith, E. C., & Holman, A. B. (1984). Satellite Anomalous from Galactic Cosmic Rays. *IEEE Trans. Nucl. Sci.*, NS-22, 2675-2680.

[7] Dodd, P. E., Musseau, O., Shaneyfelt, M. R., Sexton, F. W., D'hose, C., Hash, G. L., Martinez, M., Loemker, R. A., Leray, J-L., & Winokur, P. S. (1988). Impact of Ion Energy on Single-Event Upset. *IEEE Trans. Nucl. Sci.*, 45, 2483-2491.

[8] Sexton, F. W. (2003). Destructive Single-Event Effects in Semiconductor Devices and ICs. *IEEE Trans. Nucl. Sci.*, 50, 603-621.

[9] McWhorter, P. J., & Winokur, P. S. (1986). Simple Technique for Separating the Effects of Interface Traps and Trapped-Oxide Charge in Metal-Oxide-Semiconductor Transistors. *Appl. Phys. Lett.*, 48, 133-135.

[10] Sexton, F. W., & Schwank, J. R. (1985). Correlation of Radiation Effects in Transistors and Integrated Circuits. *IEEE Trans. Nucl. Sci.*, NS-32, 3975-3981.

[11] Ohshima, T., Morita, Y., Nashiyama, I., Kawasaki, O., Hisamatsu, T., Nakao, T., Wakow, Y., & Matsuda, S. (1996). Mechanism of Anomalous Degradation of Silicon Solar Cells Subjected to High-Fluence Irradiation. *IEEE Trans. Nucl. Sci.*, 43, 2990-2997.

[12] Ymamaguchi, M. (2001). Radiation-Resistant Solar Cells for Space Use. *Sol. Energy Mater. Sol. Cells.*, 68, 31-53.

[13] Imaizumi, M., Sumita, T., Kawakita, S., Aoyama, K., Anzawa, O., Aburaya, T., Hisamatsu, T., & Matsuda, S. (2005). Results of Flight Demonstration of Terrestrial Solar Cells in Space. *Prog. Photovolt: Res. Appl.*, 13, 93-102.

[14] Sato, S., Ohshima, T., & Imaizumi, M. (2009). Modeling of Degradation Behavior of InGaP/GaAs/Ge Triple-Junction Space Solar Cell Exposed to Charged Particles. *J. Appl. Phys.*, 105, 044504-1-6.

[15] Brew, J. R. (1981). *Applied Solid State Science.*, ed. Dawon Kahhny. Academic: New York.

[16] Ohshima, T., Yoshikawa, M., Itoh, H., Aoki, Y., & Nashiyama, I. (1999). Gamma-ray Irradiation Effects on 6H-SiC MOSFET. *Mater. Sci. & Engineer. B*, 480, 61-62.

[17] Ohshima, T., Itoh, H., & Yoshikawa, M. (2001). Effect of Gamma-ray Irradiation on the Characteristics of 6H Silicon Carbide Metal-Oxide-Semiconductor Field Effect Transistor with Hydrogen-Annealed Gate Oxide. *J. Appl. Phys.*, 90, 3038-3041.

[18] Yoshikawa, M., Saitoh, K., Ohshima, T., Itoh, H., Nashiyama, I., Takahashi, Y., Ohnishi, K., Okumura, H., & Yoshida, Si. (1998). Generation Mechanisms of Trapped Charges in Oxide Layers of 6H-SiC MOS Structures Irradiated with Gamma-Rays. *Mater. Sci. Forum*, 264-268, 1017-1020.

[19] Ohshima, T., Yoshikawa, M., Itoh, H., Kojima, K., Okada, S., & Nashiyama, I. (2000). Influence of Post-Oxidation Annealing on Electrical Characteristics in 6H-SiC MOSFETs. *Mater. Sci. Forum*, 338-342, 1299-1302.

[20] Yoshikawa, M., Saitoh, K., Ohshima, T., Itoh, H., Nashiyama, I., Yoshida, S., Okumura, H., Takahashi, Y., & Ohnishi, K. (1996). Depth Profile of Trapped Charges in Oxide Layer of 6H-SiC Metal-Oxide-Semiconductor Structures. *J. Appl. Phys.*, 80, 282-287.

[21] Hornetz, B., Michel, H. J., & Halbritter, J. (1994). ARXPS Studies of SiO2SiC Interfaces and Oxidation of 6H SiC Single-Crystal Si-(001) and C-(001) Over-Bar Surfaces. *J. Mater. Res.*, 9, 3088-3094.

[22] Schorner, R., Friedrichs, P., & Peters, D. (1999). Detailed Investigation of n-Channel Enhancement 6H-SiC MOSFET's. *IEEE Trans. Electron Devices*, 46, 533-541.

[23] Hishiki, S., Iwamoto, N., Ohshima, T., Itoh, H., Kojima, K., & Kawano, K. (2009). Effects of Fabrication Process on the Electrical Characteristics of n-channel MOSFETs Irradiated with Gamma-Rays. *Mater. Sci. Forum*, 600-603, 707-710.

[24] Negoro, Y., Katsumonot, K., Kimoto, T., & Matsunami, H. (2004). Electronic Behaviors of High-Dose Phosphorus-Ion Implanted 4H-SiC(0001). *J. Appl. Phys.*, 96, 224-228.

[25] Tanaka, Y., Onoda, S., Takatsuka, A., Ohshima, T., & Yatsuo, T. (2010). Radiation Hardness Evaluation of SiC-BGSIT. *Mater. Sci. Forum*, 645-648, 941-944.

[26] Onoda, S., Iwamoto, N., Ono, S., Katakami, S., Arai, M., Kawano, K., & Ohshima, T. (2009). Transient Response of Charge Collection by Single Ion Strike in 4H-SiC MESFETs. *IEEE Trans. Nucl. Sci.*, 56, 3218-3222.

[27] Tanaka, Y., Yano, K., Okamoto, M., Takatsuka, A., Fukuda, K., Kasuga, M., Arai, K., & Yatsuo, T. (2006). Fabrication of 700 V SiC-SIT with Ultra-Low On-Resistance of 1.01 mΩcm^2. *Mater. Sci. Forum*, 527-529, 1219-1222.

[28] Tanaka, Y., Okamoto, M., Takatsuka, A., Arai, K., Yatsuo, T., Yano, K., & Kasuga, M. (2006). 700-V 1.0-m Ωcm^2 buried gate SiC-SIT (SiC-BGSIT). *IEEE Electron Device Lett.*, 27, 908-910.

[29] Gover, J. E., & Srour, J. R. (1986). Basic Radiation Effects in Nuclear Power Electronics Technology. *Sandia Natinal Labs Report SAND85-0776*.

[30] Nava, F., Vittone, E., Vanni, P., Verzellesi, G., Fuochi, P. G., Lanzieri, C., & Glaser, M. (2003). Radiation Tolerance of Epitaxial Silicon Carbide Detectors for Electrons, Protons and Gamma-rays. *Nucl. Instr. and Meth. A*, 505, 645-655.

[31] Bertuccio, G. (2005). Prospect for Energy Resolving X-ray Imaging with Compound Semiconductor Pixel Detectors. *Nucl. Instr. and Meth. A*, 546, 232-241.

[32] Lees, J. E., Bassford, D. J., Fraser, G. W., Horsfall, A. B., Vassilevski, K. V., Wright, N. G., & Owens, A. (2007). Semi-Transparent SiC Schottky Diodes for X-ray Spectroscopy. *Nucl. Instr. Meth. A*, 578, 226-234.

[33] Giudice, A. Lo., Fasolo, F., Durisi, E., Manfredotti, C., Vittone, E., Fizzotti, F., Zanini, A., & Rosi, G. (2007). Performances of 4H-SiC Schottky Diodes as Neutron Detectors. *Nucl. Instr. Meth. A*, 583, 177-180.

[34] Flammang, R. W., Seidel, J. G., & Ruddy, F. H. (2007). Fast Neutron Detection with Silicon Carbide Semiconductor Radiation Detectors. *Nucl. Instr. Meth. A*, 578, 177-179.

[35] Ohshima, T., Satoh, T., Oikawa, M., Yamakawa, T., Onoda, S., Wakasa, T., Laird, J. S., Hirao, T., Kamiya, T., Itoh, H., Kinoshita, A., Tanaka, R., Nakano, I., Iwami, M., & Fukushima, Y. (2005). Characterization of Charge Generated in Silicon Carbide n^+p Diodes using Transient Ion Beam-Induced Current. *Nucle. Instrum. Meth. A*, 541, 236-240.

[36] Ohshima, T., Satoh, T., Oikawa, M., Onoda, S., Hishiki, S., Hirao, T., Kamiya, Yokoyama T., Sakamoto, A., Tanaka, R., Nakano, I., Wagner, G., & Itoh, H. (2007). Degradation of Charge Collection Efficiency Obtained for 6H-SiC n^+p Diodes Irradiated with Gold Ions. *Mater. Sci. Forum*, 556-557, 913-916.

[37] Onoda, S., Ohshima, T., Hirao, T., Hishiki, S., Iwamoto, N., Kojima, K., & Kawano, K. (2009). Transient Response to High Energy Heavy Ions in 6H-SiC n^+p Diodes. *Mater. Sci. Forum*, 600-603, 1039-1042.

[38] Onoda, S., Iwamoto, N., Murakami, M., Ohshima, T., Hirao, T., Kojima, T., Kawano, K., & Nakano, I. (2009). Charge Collection Properties of 6H-SiC Diodes by Wide Variety of Charged Particles up to Several Hundreds MeV. *Mater. Sci. Forum*, 615-617, 861-864.

[39] Ohshima, T., Iwamoto, N., Onoda, S., Kamiya, T., & Kawano, K. (2009). Comparative Study of Transient Current induced in SiC p+n and n+p Diodes by Heavy Ion Micro Beams. *Nucl. Instrum. Meth. B*, 267, 2189-2192.

[40] Ohshima, T., Iwamoto, N., Onoda, S., Wagner, G., Itoh, H., & Kawano, K. (2011). Charge Generated in 6H-SiC n^+p Diodes by MeV Range Heavy Ions. *Surface & Coatings Tech.*, 206, 864-868.

[41] Hirao, T., Nashiyama, I., Kamiya, T., & Nishijima, T. (1995). Effects of Micro-Beam Induced Damage on Single-Event Current Measurements. *Nucl. Instr. Meth. B*, 104, 508-514.

[42] Japan Atomic Energy Agency. (2012). *Takasaki Advanced Radiation Research Institute*, http://www.taka.jaea.go.jp/index_e.html, accessed 1 July.

[43] Laird, J. S., Hirao, T., Mori, H., Onoda, S., Kamiya, T., & Itoh, H. (2000). Development of a New Data Collection System and Chamber for Microbeam and Laser Investigations of Single Event Phenomena. *Nucl. Instr. Meth. B*, 181, 87-94.

[44] Iwamoto, N., Onoda, S., Makino, T., Ohshima, T., Kojima, K., Koizumi, A., Uchida, K., & Nozaki, S. (2011). Transient Analysis of an Extended Drift Region in a 6H-SiC Diode Formed by a Single Alpha Particle Strike and Its Contribution to the Increased Charge Collection. *IEEE Trans Nucl. Sci.*, 58, 305-313.

[45] Ziegler, J. F., Biersack, J. P., & Ziegler, M. D. (2008). *SRIM, The Stopping and Range of Ions in Matter*, SRIM Co., Chester, Maryland, USA.

[46] Zajic, V., & Thieberger, P. (1999). Heavy Ion Linear Energy Transfer Measurements during Single Event Upset Testing of Electronic Devices. *IEEE Trans. Nucl. Sci.*, 46, 59-69.

[47] Kobetich, E. J., & Katz, R. (1968). Energy Deposition by Electron Beams and δ Rays. *Phy. Rev.*, 170, 391-396.

[48] Fageeha, O., Howard, J., & Block, R. C. (1994). Distribution of Radial Energy Deposition around the Track of Energetic Charged-Particles in Silicon. *J. Appl. Phys.*, 75, 2317-2321.

[49] Ohshima, T., Iwamoto, N., Onoda, S., Makino, T., Deki, M., & Nozaki, S. (2011). Refreshable Decrease In Peak Height Of Ion Beam Induced Transient Current From Silicon Carbide Metal-Oxide-Semiconductor Capacitors. *AIP conference proceedings 1336: Application of Accelerators in Research and Industry: 21th International Conference.*, August, Fort Worth, Texas, USA, 660-664.

[50] Ohshima, T., Iwamoto, N., Onoda, S., Makino, T., Nozaki, S., & Kojima, K. (2011). Oxygen Ion Induced Charge in SiC MOS Capacitors Irradiated with Gamma-rays. *Mater. Sci. Forum*, 679-680370-373.

[51] Makino, T., Iwamoto, N., Onoda, S., Ohshima, T., Kojima, K., & Nozaki, S. (2012). Peak Degradation of Heavy-Ion Induced Transient Currents in 6H-SiC MOS Capacitors. *Mater. Sci. Forum*, 717-720469-472.

[52] Onoda, S., Makino, T., Iwamoto, N., Vizkelethy, G., Kojima, K., Nozaki, S., & Ohshima, T. (2010). Charge Enhancement Effects in 6H-SiC MOSFETs Induced by Heavy Ion Strike. *IEEE Trans. Nucl. Sci.*, 57, 3373-3379.

[53] Onoda, S., Ohshima, T., Hirao, T., Mishima, K., Hishiki, S., Iwamoto, N., Kojima, K., & Kawano, K. (2007). Decrease of Charge Collection due to Displacement Damage by Gamma Rays in a 6H-SiC diode. *IEEE Trans. Nucl. Sci.*, 54, 1953-1960.

[54] Onoda, S., Iwamoto, N., Hirao, T., Kawano, K., Kojima, K., & Ohshima, T. (2009). Reduction of Effective Carrier Density and Charge Collection Efficiency in SiC Devices due to Radiations. *AIP conference proceedings 1099: Application of Accelerators in Research and Industry: 20th International Conference*, 10-15 August 2008, Fort Worth, Texas, USA, 1010-1013.

[55] Iwamoto, N., Onoda, S., Ohshima, T., Kojima, K., Koizumi, A., Uchida, K., & Nozaki, S. (2010). Charge Collection Efficiency of 6H-SiC P^+N Diodes Degraded by Low-Energy Electron Irradiation. *Mater. Sci. Forum*, 645-648921-924.